Refractive Power and Biometric Properties of the Nonhuman Primate Isolated Crystalline Lens

David Borja,[1,2] *Fabrice Manns,*[1,2] *Arthur Ho,*[3,4,5] *Noel M. Ziebarth,*[1,2] *Ana Carolina Acosta,*[1] *Esdras Arrieta-Quintera,*[1] *Robert C. Augusteyn,*[3,4,5] *and Jean-Marie Parel*[1,2,5,6]

Purpose. To characterize the age dependence of shape, refractive power, and refractive index of isolated lenses from nonhuman primates.

Methods. Measurements were performed on ex vivo lenses from cynomolgus monkeys (cyno: $n = 120$; age, 2.7–14.3 years), rhesus monkeys ($n = 61$; age, 0.7–13.3 years), and hamadryas baboons (baboon: $n = 16$; age, 1.7–27.3 years). Lens thickness, diameter, and surface curvatures were measured with an optical comparator. Lens refractive power was measured with a custom optical system based on the Scheiner principle. The refractive contributions of the gradient, the surfaces, and the equivalent refractive index were calculated with optical ray-tracing software. The age dependence of the optical and biometric parameters was assessed.

Results. Over the measured age range isolated lens thickness decreased (baboon: −0.04, cyno: −0.05, and rhesus: −0.06 mm/y) and equatorial diameter increased (logarithmically for the baboon and rhesus, and linearly for cyno: 0.07 mm/y). The isolated lens surfaces flattened and the corresponding refractive power from the surfaces decreased with age (−0.33, −0.48, and −0.68 D/y). The isolated lens equivalent refractive index decreased (only significant for the baboon, −0.001 D/y), and as a result the total isolated lens refractive power decreased with age (baboon: −1.26, cyno: −0.97, and rhesus: −1.76 D/y).

Conclusions. The age-dependent trends in the optical and biometric properties, growth, and aging, of nonhuman primate lenses are similar to those of the pre-presbyopic human lens. As the lens ages, the decrease in refractive contributions from the gradient refractive index causes a rapid age-dependent decrease in maximally accommodated lens refractive power. (*Invest Ophthalmol Vis Sci.* 2010;51:2118–2125) DOI:10.1167/iovs.09-3905

Nonhuman primates have been used as models for myopia, emmetropization, and accommodation.[1–8] Monkeys are the only species that are known to accommodate like humans. Most notably, the accommodative apparatus and age-dependent changes in the accommodative ability of the rhesus monkey have been shown to be similar to those of humans.[3–12] For these reasons, several intraocular implants and surgical procedures to correct presbyopia are being evaluated in cynomolgus and rhesus monkeys.[13–16]

Despite general similarities in relative refractive contribution from the lens to total ocular power, there are key interspecies differences in lens shape and refractive power between humans and monkeys.[8] For instance, monkey lenses can have a smaller diameter, steeper curvatures, and higher refractive power than human lenses of comparable ages.[8] It has been suggested that there may be different underlying causes of presbyopia in monkeys and humans due to species differences in lens growth and ciliary body aging.[17] Since the monkey eye is often used as a model for the human eye in physiological optics, it is important to precisely quantify the optical and biometric properties of the monkey eye and to better characterize the interspecies differences. Of particular importance for studies on presbyopia and accommodation is a thorough understanding of the properties of the lens and its changes with age.

There have been several biometric studies on rhesus monkey lens diameter, thickness, and surface curvatures,[3,8,12] but there is large variability in the reported optical and biometric properties.[5,8] There are few published studies on the optical and biometric properties of lenses from other nonhuman primate species, such as baboons. To our knowledge, there have been no direct measurements of either the isolated lens shape or refractive power of the nonhuman primate over a wide age range. In a previous study conducted on isolated human lenses, we demonstrated that age-dependent changes in the gradient refractive index are a major contributor to the decrease in isolated lens refractive power with age. This decrease was found to correspond well with the loss of in vivo accommodative ability.[18] From the literature it is not clear whether the nonhuman primate undergoes similar age-dependent changes.

The purpose of this study was to characterize the shape and the optical properties of isolated lenses from the rhesus monkey, cynomolgus monkey, and hamadryas baboon as a function of age. The results are compared to those from a similar study on isolated human lenses.[18,19]

From the [1]Ophthalmic Biophysics Center, Bascom Palmer Eye Institute, University of Miami Miller School of Medicine, Miami, Florida; the [2]Biomedical Optics and Laser Laboratory, Department of Biomedical Engineering, University of Miami, Coral Gables, Florida; the [3]Institute for Eye Research, Sydney, NSW, Australia; the [4]School of Optometry and Vision Science, University of New South Wales, Sydney, NSW, Australia; the [5]Vision Cooperative Research Centre, Sydney, Australia; and the [6]CHU Department of Ophthalmology, University of Liège CHU Sart-Tillmann, Liège, Belgium.

Supported in part by National Institutes of Health Grants 2R01EY14225, 5F31EY15395; an NRSA Individual Predoctoral Fellowship [DB]); a National Science Foundation (NSF) Graduate Fellowship (NMZ); the Australian Federal Government Cooperative Research Centres Programme through the Vision Cooperative Research Centre; the Florida Lions Eye Bank; P30EY14801 (Center Grant); an unrestricted grant from Research to Prevent Blindness (JMP); and the Henri and Flore Lesieur Foundation (JMP).

Submitted for publication April 24, 2009; revised July 20, 2009; accepted October 23, 2009.

Disclosure: **D. Borja**, None; **F. Manns**, None; **A. Ho**, None; **N.M. Ziebarth**, None; **A.C. Acosta**, None; **E. Arrieta-Quintera**, None; **R.C. Augusteyn**, None; **J.-M. Parel**

Corresponding author: Fabrice Manns, Bascom Palmer Eye Institute, 1638 NW 10 Avenue, Miami, FL 33136; fmanns@miami.edu.

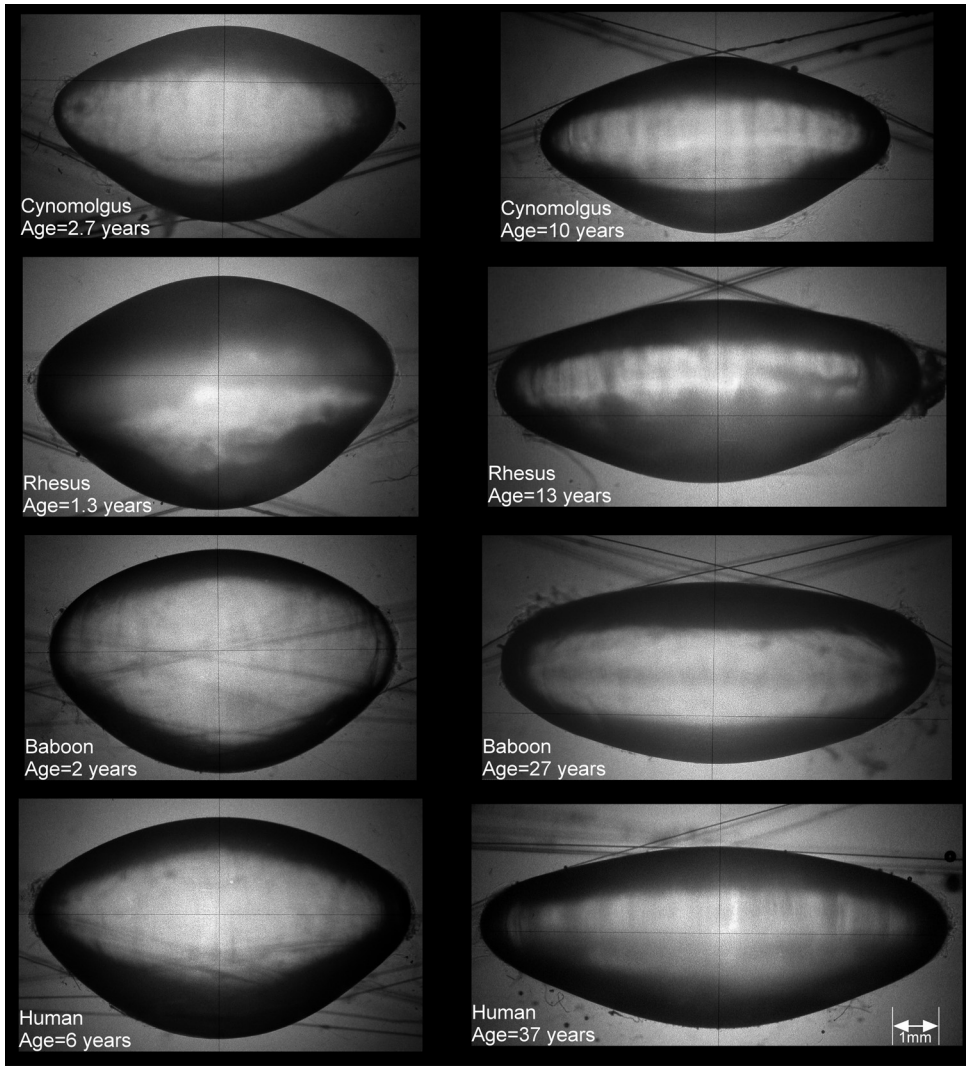

FIGURE 1. Sample sagittal (side view) shadowgraph images of young (*left*) and older (*right*) lenses from cynomolgus monkeys, rhesus monkeys, and hamadryas baboons. Shadowgraphs of young and older human lenses obtained from a previous study are included for reference.[18] All images are at the same scale and show the crosshairs of the optical comparator and the supporting suture mesh of the immersion cell.

MATERIALS AND METHODS

General Description

The refractive power and shape of ex vivo nonhuman primate crystalline lenses were measured and used to calculate the refractive contributions of the lens surfaces and the refractive index gradient by using published techniques.[18–21] Briefly, the refractive power was measured with a custom-designed optical system based on the Scheiner principle while the lens was maintained in its accommodative framework and mounted in the testing cell of a lens-stretching system under no applied tension.[18,21] This system delivers four parallel laser beams (with a diameter of 300 μm) arranged in a 3-mm-square pattern through the crystalline lens. A camera mounted on an adjustable vertical translation stage is used to detect the location of convergence of the four beams. This location corresponds to the focal plane of the lens. The refractive power of the lens immersed in the testing chamber is calculated by using a formula derived from a paraxial optical model of the system. The Scheiner system was calibrated on a set of plano convex glass lenses in the power range of 10 to 45 D. The measurement error ranged from −1.8 to 2.9 D (average, 1.5 D).[18] A separate preliminary study showed that the shape and refractive power of the unstretched crystalline lens are not affected by stretching experiments (Parel JM, et al. *IOVS* 2002;43:ARVO E-Abstract 406). The shape of the isolated lens was measured from undistorted magnified sagittal profile images obtained with a modified optical comparator (Fig. 1). The comparator produces digital shadowgraph images of the isolated crystalline lens at 20× magnification.[20,22] During these measurements the lens was supported by a meshwork of 10-0 nylon monofilament sutures in an immersion chamber filled with DMEM. The central lens thickness (t) and equatorial diameter (d), as well as the anterior and posterior surface profiles,[20] were obtained from the shadowgraph images (Fig. 1). The surface profiles were fit with conic functions over the central 6-mm zone, to calculate the radii of curvatures (R) and asphericities (Q).[20,23] The accuracy of the surface curvature measurement was quantified by using a stainless steel ball bearing with $R = 4.763$ mm. The measurement error was 0.9% for the radius of curvature and 5% for the asphericity. The accuracy of the thickness and diameter measurement estimated on the same calibration sphere was ± 12 μm.

For each lens, the refractive contributions of the surfaces and the refractive index gradient to the measured lens refractive power were then calculated by using optical ray-tracing software (OSLO LT; Lambda Research, Littleton, MA).[18] In this study the measured lens shape and refractive power both corresponded to that of the maximally accommodated lens under no external forces. The age dependence of the optical and biometric parameters were assessed and compared to those of the human lens.

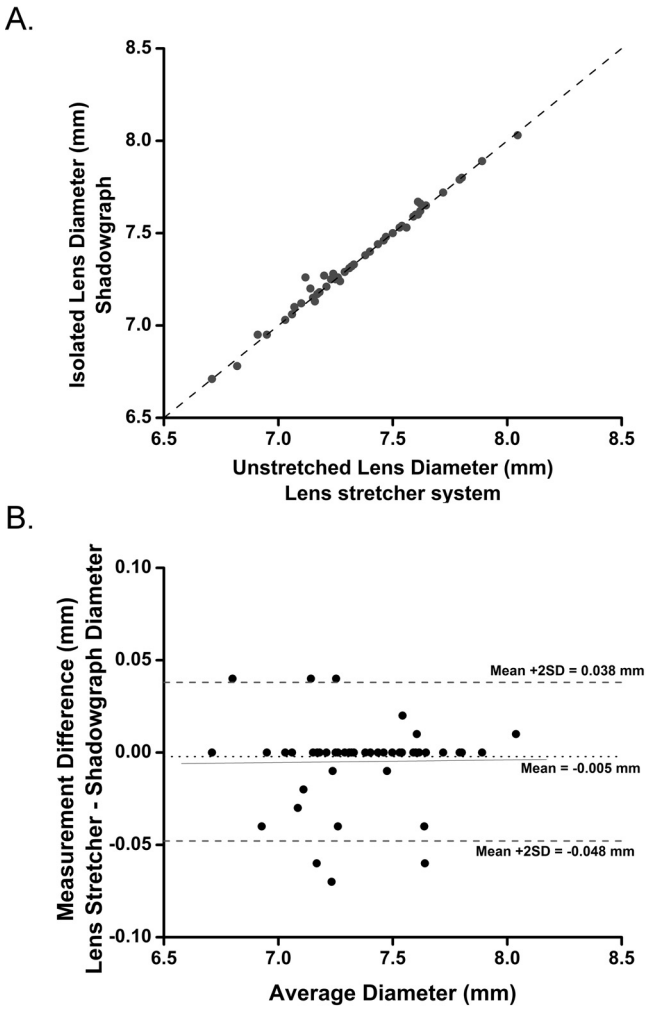

FIGURE 2. (**A**) The cynomolgus monkey isolated lens diameter plotted against the unstretched lens diameter for the same lens measured in the lens-stretching system. (**B**) A Bland-Altman analysis was performed to determine whether both systems produced comparable results. This analysis determined that in the cynomolgus monkey there was no significant difference ($P = 0.9$) between the unstretched lens diameter measured in the lens stretcher (mean, 7.35 ± 0.29 mm) and the isolated lens diameter (mean, 7.36 ± 0.28 mm) measured in the optical comparator (shadowgraph system). Similar results were found for human lenses in a previous study (Ho A, et al. *IOVS* 2007;48:E-Abstract 3816), and similar results were expected from the baboon and the rhesus monkey lenses.

Donor Tissue

All animal experiments adhered to the ARVO Statement for the Use of Animals in Ophthalmic and Visual Research. No animal was killed for the sole purpose of this study. Whole eyes of rhesus and cynomolgus monkeys and hamadryas baboons were obtained through the Division of Veterinary Resources at the University of Miami as part of a university-wide tissue-sharing protocol and were used in accordance with institutional animal care and use guidelines.

Refractive power was measured on 120 ex vivo lenses from 89 donor cynomolgus monkeys (*Macaca fascicularis*: postmortem time [PMT], 11.8 ± 13.7 hours; age, 2.7–14.3 years); on 61 ex vivo lenses from 40 donor rhesus monkeys (*Macaca mulatta*: PMT, 22.3 ± 14.9 hours; age, 0.7–13.3 years); and on 16 ex vivo lenses from 16 donor hamadryas baboons (*Papio hamadryas*; PMT, 12.1 ± 14.8 hours; ages, 1.7–27.3 years) all obtained within 24 hours of euthanization. Some of the lenses had been used for other experiments and therefore could not be prepared for lens shape measurements in the optical comparator after the power was measured. In total, lens shape was measured on 76 lenses from 58 cynomolgus monkeys, 43 lenses from 23 rhesus monkeys, and 16 lenses from 13 hamadryas baboons. Any lens with visible damage on shadow photogrammetry imaging was excluded from the analysis. In total, 8 lenses (0 rhesus, 1 baboon, and 7 cynomolgus monkey lenses) of a total of 135 lenses placed in the shadowgraph had to be excluded due to damage or swelling.

Tissue Dissection

Dissections were performed by ophthalmic surgeons under a motorized operation microscope (OMS-300; Topcon, Tokyo, Japan). A complete description of the tissue preparation protocol can be found in another publication.[21] In this technique a band of eight independent shoes, matching the scleral curvature, were bonded with cyanoacrylate adhesive (Duro SuperGlue; Henkel Locktite Corp., Cleveland, OH) onto the anterior sclera surface from the limbus to the equator. This method prevents deformation of the globe during dissection, and the shoes provide attachment for a lens-stretching device. The posterior pole was then sectioned, and scleral incisions were made between adjacent shoes followed by removal of the cornea and iris to produce eight individual segments for stretching. The tissue section including the lens was mounted in the testing chamber of the lens stretcher, and refractive power was measured in lenses in the unstretched state. The testing chamber of the lens stretcher was filled with preservative medium (DMEM/F-12, D8437; Sigma-Aldrich, St. Louis, MO) to prevent swelling.[24]

On average, the lens was immersed in DMEM for approximately 30 minutes until the refractive power measurements were completed. At the end of the stretching experiments, the lens was extracted by carefully cutting the zonules and adherent vitreous with Vannas scissors. The isolated lens was immediately immersed in a DMEM-filled vial to prevent swelling.[24] The vial was then placed in the optical comparator for lens shape measurements. In total, the lenses were immersed in DMEM for ~1 to 2 hours during the stretching experiments in the apparatus before shadowgraph measurements of the isolated lens shape.

Data and Statistical Analysis

Previous studies have shown that there is no significant difference between the diameter and the refractive power of the isolated lens and

FIGURE 3. Thickness and diameter of in vitro isolated hamadryas baboon, cynomolgus monkey, and rhesus monkey lenses as a function of age. A nonlinear growth rate was observed for the isolated lens diameter in the rhesus monkey and hamadryas baboon which were modeled with a logarithmic function (Table 2).

TABLE 1. Age-Dependent Linear and Nonlinear Regression Equations of the Measured Nonhuman Primate In Vitro Lens Biometric Properties

Species	Hamadryas Baboon	Cynomolgus Monkey	Rhesus Monkey
Age range, y	1.67–27.3	1.7–14.3	0.7–13.3
Central thickness, mm	4.64-0.04 · Age $P = 0.002$	4.33–0.05 · Age $P < 0.0001$	4.90–0.06 · Age $P < 0.0001$
Equatorial diameter, mm	7.16 ± 0.50 · ln(Age) $P < 0.0001$	6.92 ± 0.07 · Age $P < 0.0001$	7.42 ± 0.53 · ln(Age) $P < 0.0001$
Approximate volume mm^3	140.5 ± 1.24 · Age $P = 0.003$	112.59 ± 8.12 $P = 0.14$	135.9 ± 14.9 · ln(Age) $P < 0.0001$

The averages and SD are given for the parameters which showed no statistically significant age dependency.

the lens mounted in the lens stretcher under no tension[18] (Ho A, et al. *IOVS* 2007;48:E-Abstract 3816). In these experiments, top views of the lens mounted in the lens stretcher were recorded with a digital camera mounted on an operation microscope set at 10× magnification.[21] A Bland-Altman analysis was performed to determine whether both systems produced comparable results. The findings of this analysis are presented in the Results section.

There was no significant difference ($P < 0.05$) in the biometric and optical properties between lenses obtained from the eyes of the same donor. Therefore, to prevent values obtained from paired eyes from biasing the statistics for age dependence, the values from the eyes of each donor were averaged. The average values were then used as a single point for age-dependence calculations.

The lens volume was estimated by assuming that the lens was a rotationally symmetric ellipsoid with a long axis equal to the equatorial diameter and a short axis equal to the lens thickness.[20] This ellipsoid model was used as an approximation for the whole lens shape, including the equatorial region, only for the calculation of volume, whereas the conic fits were used to obtain more accurate values of the radius of curvature and asphericity of the lens in the central 6-mm diameter zone. The surface radii of curvature and asphericity are reported with positive values for the anterior surface and negative values for the posterior surface.

The refractive contributions of the lens surfaces were determined by calculating the refractive power of each lens, assuming a uniform refractive index equal to the outer cortex refractive index ($n_{surfaces} = 1.371$).[25] The contribution of the refractive index gradient is expressed as an equivalent refractive index, which is the uniform refractive index value required inside the lens to provide a refractive power equal to the measured lens refractive power.

The biometric (central thickness, equatorial diameter, and surface radii of curvatures) and optical properties (refractive power, surface contribution, and equivalent refractive index) were plotted as a function of age. Linear and nonlinear regressions were calculated for each data plot to determine whether there was an age dependence. A logarithmic growth function was used to model the growth of the isolated lens dimensions which displayed a nonlinear age dependence. $P \leq 0.05$ was set as the condition for statistical significance.

RESULTS

Isolated nonhuman primate lenses displayed an increase in equatorial diameter, a decrease in thickness, a flattening of the surfaces (Fig. 1), and a decrease in equivalent refractive index, leading to a dramatic age-dependent decrease in refractive power of the isolated lens.

In this study, refractive power measurements were obtained while the lenses were mounted in a lens-stretching apparatus. Figure 2 shows the cynomolgus monkey isolated lens diameter versus the unstretched lens diameter measured in the lens-stretching system. A Bland-Altman analysis performed on these results determined that there was no significant difference ($P = 0.9$) between the unstretched lens diameter measured in the lens-stretching system (mean diameter,

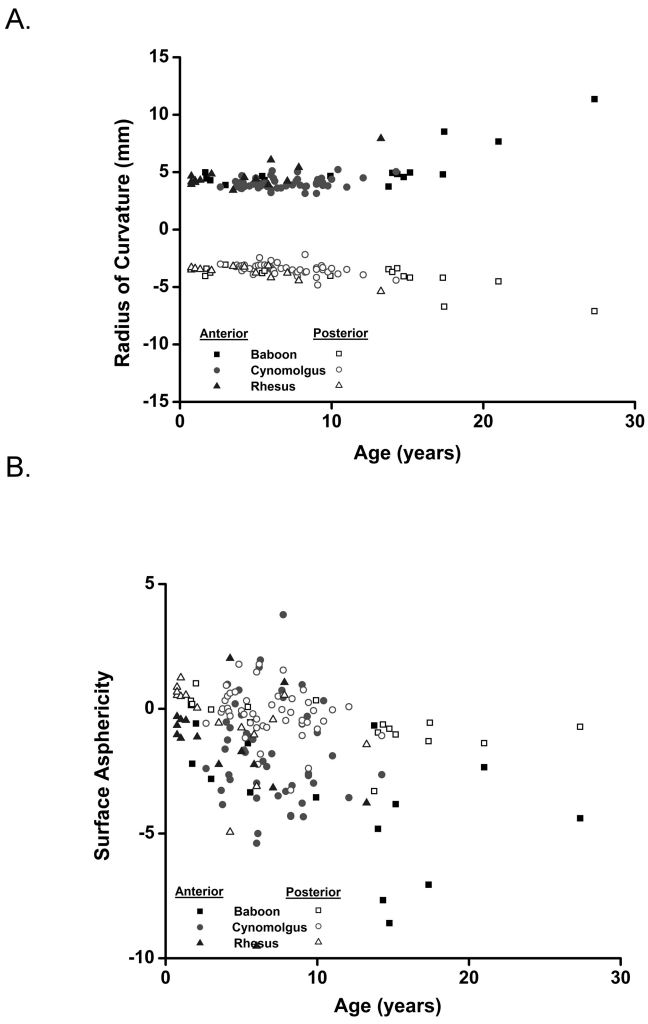

FIGURE 4. Anterior and posterior surface curvatures (**A**) and surface asphericities (**B**) of isolated hamadryas baboon, cynomolgus monkey, and rhesus monkey lenses as a function of age. A nonlinear trend was observed for the baboon lens anterior radius of curvature (Table 2). With age, the asphericity became more negative ($Q < 0$), which corresponds to a hyperbolic shape.

7.35 ± 0.29 mm) and that of the isolated lens (mean diameter, 7.36 ± 0.28 mm), when measured by the optical comparator (shadowgraph).

The examples of isolated crystalline lens shadowgraphs in Figure 1 illustrate the growth of the crystalline lens in all three nonhuman primate species. Lens dimensions are shown in Figure 3. Regression analyses are summarized in Table 1. Nonlinear age-dependent trends were observed for isolated lens diameter growth in the nonhuman primates as well as for the anterior surface curvatures in the hamadryas baboon. The central lens thickness of all three species decreased linearly ($P < 0.05$) throughout the measured age ranges (Table 1). The measured lens refractive power and calculated surface refractive power both decreased linearly over the sampled age ranges. Linear age-dependent trends were also observed with the hamadryas baboon lens for surface refractive contribution and equivalent refractive index.

The approximate volume of the isolated rhesus monkey lens, calculated from the measured dimensions, displayed logarithmic growth in the measured age range. The lenses of the cynomolgus monkeys are smaller in diameter and slightly thicker than comparably aged hamadryas baboon and rhesus monkey lenses. They are also slightly smaller in total volume than the other nonhuman primate species.

The anterior and posterior radii of curvature for all three nonhuman primate species increased (flattening) with age (Fig. 4, Table 2). In the hamadryas baboon the anterior surface curvature increased nonlinearly over the age range of 1.7 to 27.3 years. It remained constant until approximately 15 years of age and then started to increase. In the rhesus monkey, the anterior lens surface curvature showed an age-dependent increase; however, the trend was not statistically significant. The surface curvatures of the cynomolgus monkey lens appeared to increase linearly throughout the sampled age range.

Over the age range examined, lens refractive power decreased in all three species (Fig. 5, Table 3). In the baboon, in absolute values, surface refractive power (0.33 D/y) decreased at a considerably slower rate than the refractive power (1.26 D/y) (Fig. 5, Table 3). Consequently, in the baboon, the refractive contribution of the surfaces, as a percentage of the refractive power, increased with age (+0.62%/y; Fig. 6), and the equivalent refractive index decreased with age (−0.001/year; Fig. 7). This age-dependent decrease in equivalent refractive index is due to a decrease in the refractive contribution from the gradient refractive index. Similar trends were observed in the relative surface refractive contributions and in the equivalent refractive index for the rhesus and the cynomolgus monkeys; however, these trends were not significant, probably because of the smaller age ranges of the cynomolgus and rhesus monkey lenses that were available for the study, as well as the high variability of the data.

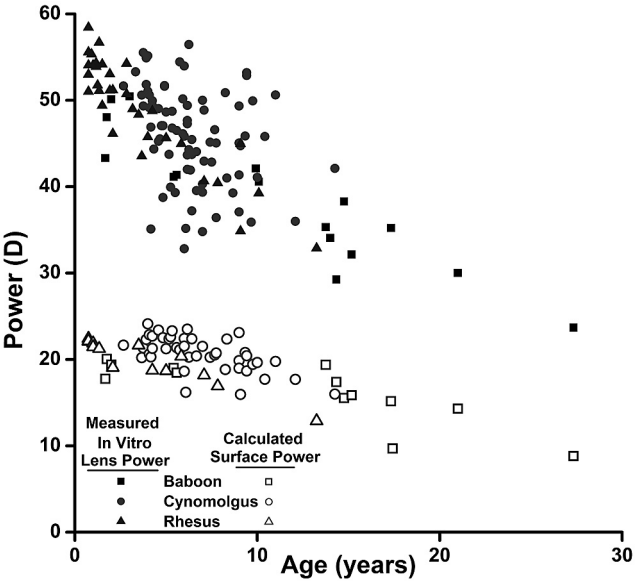

FIGURE 5. Measured refractive power and calculated surface refractive power of in vitro hamadryas baboon, cynomolgus monkey, and rhesus monkey lenses as a function of age. The measured refractive power decreased linearly in all three species with age (Table 3).

DISCUSSION

In this study, the biometric and optical properties of a large sample of fresh in vitro nonhuman primate lenses were measured, most within hours of euthanatization. The main advantage of in vitro measurement is that it allows for direct measurement of lens refractive power. However, there are

TABLE 2. Age-Dependent Regression Equations of the Measured Nonhuman Primate In Vitro Lens Biometric Properties

Species	Hamadryas Baboon	Cynomolgus Monkey	Rhesus Monkey
Age range, y	1.7–27.3	1.7–14.3	0.7–13.3
Anterior radius of curvature, mm	$4.01 \pm 0.16\, e^{\frac{Age}{7.10}}$* $\chi^2 = 0.93$ $r^2 = 0.80$	3.66 ± 0.06 · Age $P = 0.04$	4.68 ± 1.10 $P = 0.36$
Posterior Radius of Curvature, mm	−3.03–0.09 · Age $P = 0.01$	−2.80–0.09 · Age $P < 0.001$	−3.27–0.08 · Age $P < 0.001$
Anterior surface asphericity	−0.89–0.25 · Age $P = 0.01$	−1.62 ± 1.96 $P = 0.60$	−0.98 ± 1.38 $P = 0.34$
Posterior surface asphericity	0.29–0.06 · Age $P = 0.002$	−0.11 ± 0.89 $P = 0.140$	0.52–0.23 · Age $P = 0.06$

The surface radii of curvature were measured over the central 6-mm optical zone and are reported with positive values for the anterior surface and negative values for the posterior surface. The averages ± SD are given for the parameters which showed no statistically significant age dependency.

* Over the age range of 1.7 to 15 years, the radius of curvature remains constant with an average value of 4.53 ± 0.41 mm.

TABLE 3. Age Dependence of In Vitro Nonhuman Primate Lens Optical Properties

Species	Hamadryas Baboon	Cynomolgus Monkey	Rhesus Monkey
Age range, y	1.7–27.3	2.7–14.3	0.7–13.3
Refractive power, D	52.56–1.26 · Age $P < 0.0001$	52.25–0.97 · Age $P < 0.0001$	55.17–1.76 · Age $P < 0.0001$
Calculated surface power, D	20.41–0.33 · Age $P < 0.0001$	24.03–0.48 · Age $P < 0.0001$	22.47–0.68 · Age $P < 0.0001$
Relative surface refractive contribution, %	38.40 ± 0.62 · Age $P = 0.030$	45.29 ± 5.85 $P = 0.27$	41.89 ± 2.50 $P = 0.710$
Equivalent refractive index	1.427–0.001 · Age $P = 0.02$	1.418 ± 0.009 $P = 0.38$	1.423 ± 0.005 $P = 0.41$

The averages ± SD are given for the parameters which showed no statistically significant age dependency.

several limitations of in vitro measurement of isolated lenses, as opposed to in vivo measurement. For example, in vitro measurements correspond to the maximally accommodated state, whereas in vivo measurement can be performed at various accommodative states. It is also not possible to determine the relation between the lens parameters measured in vitro and the actual accommodation response of the whole eye. The main limitation of in vitro human lens studies is that it is difficult to maintain the natural lens shape and refractive power in postmortem lenses, especially if the lenses have been stored for several days in the preservative media used by eye banks.[24] In previous studies,[24,26] we found that lenses with a postmortem time of less than 24 hours could be immersed in DMEM for as long as 5 hours without swelling, as long as the capsule was intact. Swelling occurred only in lenses that were damaged during preservation or extraction. The short postmortem times proved to be a benefit compared with similar human in vitro crystalline lens studies in which long postmortem time results in the rejection of many otherwise viable samples due to swelling.[24] As part of the experimental protocol, the high-magnification shadowgraph images are used to detect any damage or capsular detachment. In the present study, only 8 (6%) of 135 lenses imaged with the shadowgraph were found to be damaged or swollen.

In all three nonhuman primate species, we found an age-dependent flattening of the lens surfaces (Figs. 1, 4) and a decrease in refractive power (Fig. 5) which also have been observed in pre-presbyopic adult human lenses (<50 years old).[18] An approximate scaling factor of 1 monkey year to 3 human years has been used by other investigators to compare the age-dependent decrease in the human and rhesus monkey accommodative response[3] and emmetropization.[8] With this scaling factor, the nonhuman primates in this study corresponded to a human age range of 2 to 40 years. In that age range, the rate of decrease in the human lens refractive power was −0.41 D/y in our previous in vitro study.[18] This result is similar to those found in the rhesus monkey in the present study scaled for age as well as for the other two species (rhesus: −0.58 D/human year; cyno: −0.42 D/human year; baboon −0.32D/human year; Table 3). The similarities in the lens properties as well as the ease of availability and short postmortem times tends to justify the use of the nonhuman primate as a model for the human lens in in vitro accommodation and presbyopia studies.

Our results show that over the sampled age range, the refractive power of the isolated crystalline lens decreased by more than 20 D in all three species. Equatorial lens diameter increased, whereas central thickness decreased over the sampled age range in all three species. It might have been ex-

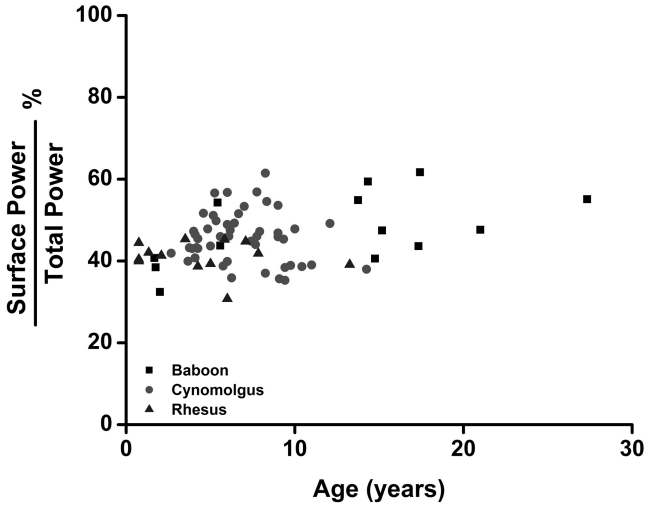

FIGURE 6. The surface contributions to the refractive power of in vitro hamadryas baboon, cynomolgus monkey, and rhesus monkey lenses as a function of age (Table 3).

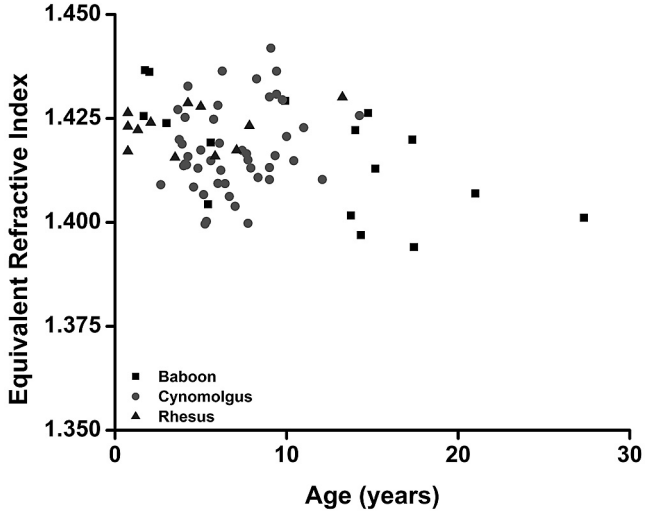

FIGURE 7. Calculated equivalent refractive index of in vitro hamadryas baboon, cynomolgus monkey, and rhesus monkey lenses as a function of age (Table 3).

pected that central lens thickness would increase in the monkey lens, similar to the human lens, which decreases in the first decade or so of life and then increases.[27] However, this trend was not observed in this study, probably because of the limited number of samples in the upper age range.

It is difficult to directly compare the lens refractive power and biometry results from this study with in vivo measurements. Typically, in vivo measurements of lens shape and refractive power are performed on the relaxed, disaccommodated lens after pharmacologic pupil dilation. The lenses included in this study were isolated and free of external forces. Their shape and refractive power were expected to correspond to those of the maximally accommodated lens which is free of zonular tension. The isolated lens growth trends observed in this study are in good agreement with results obtained on maximally accommodated rhesus monkey lenses in vivo.[5,8,12] Wendt et al.[12] found that the maximally accommodated rhesus monkey lens diameter increases with age at a rate of 0.043 mm/y, which is similar to the results reported here for the isolated lens. Other investigators have observed an age-dependent decrease in the central lens thickness of the young human and nonhuman primate during in vivo measurements.[8,27–30] A general flattening of the lens surfaces with age has been well documented in the monkey.[5,8] Recently, Rosales et al.[30] used Purkinje imaging to measure the accommodation-dependent lens radii of curvature in two 9-year-old rhesus monkeys. They found maximally accommodated radii of curvature (6.79 mm for the anterior and −5.11mm for the posterior surfaces) that were within the range of our measurements, indicating that the isolated lens is representative of the in vivo maximally accommodated lens in the nonhuman primate, as is the case in the human.

In the hamadryas baboon, as in the human lens, the decrease in refractive contribution from the internal refractive index gradient was the major contributing factor to the rapid loss of maximally accommodated lens refractive power from birth to the age range of presbyopia onset (Fig. 6).

The equivalent refractive indexes from the present study (maximum measured values of 1.436 for both cynomolgus monkey and baboon lenses and 1.430 for the rhesus monkey) are similar to those of the human lens in vivo (maximum of 1.4375)[31] and in vitro (maximum of 1.432).[18] The rhesus monkey equivalent refractive indexes from the present study are lower than previously reported in vivo values (1.447 for a 5-year-old rhesus monkey lens[8]). The higher equivalent refractive indexes reported by Qiao-Grider et al.[8] may be due to differences in accommodative state during biometric measurements. In their study the measurements of the refractive state and lens surface profiles of rhesus monkeys were performed after accommodation was pharmacologically relaxed. In the present study, the measurements correspond to the maximally accommodated state (lens free of external forces). The results from the present study indicate the similarity between humans and these three nonhuman primate species in the general value and the age-dependent trend of the equivalent refractive index.

In summary, the results of this study highlight the similarities in optical properties, biometric properties, growth, and aging of the isolated nonhuman primate lens to those of the human lens. In both human and nonhuman primates, there is a rapid age-dependent decrease in the refractive power of the maximally accommodated lens from birth up to the onset of presbyopia. The flattening of the lens surfaces in the maximally accommodated state contributes only a small portion to the age-dependent decrease in maximally accommodated lens refractive power. In both humans and nonhuman primates, the decrease in refractive contributions from the gradient refractive index is the major contributor to the rapid age-dependent decrease in maximally accommodated lens refractive power and the consequent decrease in maximum accommodative amplitude. These findings suggest that independent of the changes in lens shape, the age-dependent changes in the internal lens refractive index distribution have a significant contribution to the loss of accommodative amplitude that leads to presbyopia.

Acknowledgments

The authors thank Norma Kenyon, PhD, and Dora Berman-Weinberg, PhD, of the DRI, and Linda Waterman, PhD, of DVR for scientific support; Viviana Fernandez, MD, Christian Billotte, MD, Ali Abri MD, Mohammed Aly, MD, Hideo Yamamoto, MD, PhD, and Adriana Amelinckx, MD, for surgical support; and David Denham, MBA, Andres Bernal, MSBME, Raksha Urs, MSBME, Marcia Orozco, MSBME, Derek Nankivil, BS, Izuru Nose, BSEE, William Lee, David Chin Yee, MD, Minh Hoang, BSBME, Stephanie Delgado, BSBME, and Jared Smith, BSBME, for technical support. This study includes data that were originally acquired by Alexandre M. Rosen, MD, MSBME.

References

1. Tornqvist G. Effect of topical carbachol on the pupil and refraction in young and presbyopic monkeys. *Invest Ophthalmol Vis Sci.* 1966;5:186–195.
2. Kaufman PL, Rohen JW, Barany EH. Hyperopia and loss of accommodation following ciliary muscle disinsertion in the cynomolgus monkey physiologic and scanning electron microscopic studies. *Invest Ophthalmol Vis Sci .* 1979;18:665–673.
3. Bito LZ, DeRousseau CJ, Kaufman PL, Bito JW. Age-dependent loss of accommodative amplitude in rhesus monkeys: an animal model for presbyopia. *Invest Ophthalmol Vis Sci.* 1982;23(1):23–31.
4. Koretz JF, Neider MW, Kaufman PL, Bertasso AM, DeRousseau CJ, Bito LZ. Slit-lamp studies of the rhesus monkey eye, I: survey of the anterior segment. *Exp Eye Res.* 1987;44(2):307–318.
5. Koretz JF, Bertasso AM, Neider MW, True-Gabelt BA, Kaufman PL. Slit-lamp studies of the rhesus monkey eye, II: changes in crystalline lens shape, thickness and position during accommodation and aging. *Exp Eye Res.* 1987;45(2):317–326.
6. Koretz JF, Bertasso AM, Neider MW, Kaufman PL. Slit-lamp studies of the rhesus monkey eye, III: the zones of discontinuity. *Exp Eye Res.* 1988;46(6):871–880.
7. Glasser A, Kaufman PL. The mechanism of accommodation in primates. *Ophthalmology.* 1999;106(5):863–872.
8. Qiao-Grider Y, Hung LF, Kee CS, Ramamirtham R, Smith EL 3rd. Normal ocular development in young rhesus monkeys (Macaca mulatta). *Vision Res.* 2007;47(11):1424–1444.
9. Neider MW, Crawford K, Kaufman PL, Bito LZ. In vivo videography of the rhesus monkey accommodative apparatus: age-related loss of ciliary muscle response to central stimulation. *Arch Ophthalmol.* 1990;108:69–74.
10. Croft MA, Kaufman PL, Crawford KS, Neider MW, Glasser A, Bito LZ. Accommodation dynamics in aging rhesus monkeys. *Am J Physiol.* 1998;275:1885–1897.
11. Croft MA, Glasser A, Heatley G, et al. Accommodative ciliary body and lens function in rhesus monkeys, I: normal lens, zonule and ciliary process configuration in the iridectomized eye. *Invest Ophthalmol Vis Sci.* 2006;47:1076–1086.
12. Wendt M, Croft MA, McDonald J, Kaufman PL, Glasser A. Lens diameter and thickness as a function of age and pharmacologically stimulated accommodation in rhesus monkeys. *Exp Eye Res.* 2008;86(5):746–752.
13. Haefliger E, Parel JM, Fantes F, et al. Accommodation of an endocapsular silicone lens (Phaco-Ersatz) in the nonhuman primate. *Ophthalmology.* 1987;94(5):471–477.
14. Haefliger E, Parel JM. Accommodation of an endocapsular silicone lens (Phaco-Ersatz) in the aging rhesus monkey. *J Refract Corneal Surg.* 1994;10:550–555.

15. Nishi O, Nishi K. Accommodation amplitude after lens refilling with injectable silicone by sealing the capsule with a plug in primates. *Arch Ophthalmol.* 1998;116:1358–1361.
16. Koopmans SA, Terwee T, Glasser A, et al. Accommodative lens refilling in rhesus monkeys. *Invest Ophthalmol Vis Sci.* 2006;47:2976–2984.
17. Strenk SA, Strenk LM, Guo S. Magnetic resonance imaging of aging, accommodating, phakic, and pseudophakic ciliary muscle diameters. *J Cataract Refract Surg.* 2006;32(11):1792–1798.
18. Borja D, Manns F, Ho A, et al. Optical power of the isolated human crystalline lens. *Invest Ophthalmol Vis Sci.* 2008;49:2541–2548.
19. Urs R, Manns F, Ho A, et al. Shape of the isolated ex-vivo human crystalline lens. *Vision Res.* 2009;49:74–83.
20. Rosen AM, Denham DB, Fernandez V, et al. In vitro dimensions and curvatures of human lenses. *Vision Res.* 2006;46:1002–1009.
21. Manns F, Parel JM, Denham D, et al. Optomechanical response of human and monkey lenses in a lens stretcher. *Invest Ophthalmol Vis Sci.* 2007;48:3260–3268.
22. Denham D, Holland S, Mandelbaum S, Pflugfelder S, Parel JM. Shadow photogrammetric apparatus for the quantitative evaluation of corneal buttons. *Ophthalmic Surg.* 1989;20:794–799.
23. Manns F, Fernandez V, Zipper S, et al. Radius of curvature and asphericity of the anterior and posterior surface of human cadaver crystalline lenses. *Exp Eye Res.* 2004;78(1):39–51.
24. Augusteyn RC, Rosen AM, Borja D, Ziebarth NM, Parel JM. Biometry of primate lenses during immersion in preservation media. *Mol Vis.* 2006;12:740–747.
25. Jones CE, Atchison DA, Meder R, Pope JM. Refractive index distribution and optical properties of the isolated human lens measured using magnetic resonance imaging (MRI). *Vision Res.* 2005;45(18):2352–2366.
26. Rosen A. Biometry of the primate crystalline lens. Master's thesis. Miami, FL: University of Miami; 2003.
27. Larsen JS. The sagittal growth of the eye, II: ultrasonic measurement of the axial diameter of the lens and the anterior segment from birth to puberty. *Acta Ophthalmol.* 1971;49:427–439.
28. Zadnik K, Mutti DO, Friedman NE, Adams AJ. Initial cross-sectional results from the Orinda Longitudinal Study of Myopia. *Optom Vis Sci.* 1993;70(9):750–758.
29. Ip JM, Huynh SC, Kifley A, et al. Variation of the contribution from axial length and other oculometric parameters to refraction by age and ethnicity. *Invest Ophthalmol Vis Sci.* 2007;48(10):4846–4853.
30. Rosales P, Wendt M, Marcos S, Glasser A. Changes in crystalline lens radii of curvature and lens tilt and decentration during dynamic accommodation in rhesus monkeys. *J Vision.* 2008;8(1):1–12.
31. Dubbelman M, Van der Heijde GL. The shape of the aging human lens: curvature, equivalent refractive index and the lens paradox. *Vision Res.* 2001;41(14):1867–1877.